

# Graphene/hydroxyapatite nano-composite for enhancement of hydrogen productivity from delignified duckweed

Ahmed Tawfik<sup>a,\*</sup>, Xuefei Tan<sup>b,c,\*</sup>, Mohamed Elsamadony<sup>d</sup>, Muhammad Abdul Qyyum<sup>e</sup>, Ahmed M. Azzam<sup>f</sup>, Muhammad Mubashir<sup>g</sup>, Hui Suan Ng<sup>h</sup>, Muhammad Saeed Akhtar<sup>i,\*</sup>, Kuan Shiong Khoo<sup>j,\*</sup>

<sup>a</sup> Water Pollution Research Department, National Research Centre, 12622, Dokki, Cairo, Egypt

<sup>b</sup> College of Materials and Chemical Engineering, Heilongjiang Institute of Technology, Harbin 150050, People's Republic of China

<sup>c</sup> State Key Laboratory of Urban Water Resource and Environment, School of Environment, Harbin Institute of Technology, Harbin 150090, People's Republic of China

<sup>d</sup> Department of Public Works Engineering, Faculty of Engineering, Tanta University, 31521 Tanta City, Egypt

<sup>e</sup> Department of Petroleum & Chemical Engineering, Sultan Qaboos University, Muscat, Oman

<sup>f</sup> Environmental Research Department, Theodor Bilharz Research Institute, 12411 Cairo, Egypt

<sup>g</sup> Department of Petroleum Engineering, School of Engineering, Asia Pacific University of Technology and Innovation, 57000 Kuala Lumpur, Malaysia

<sup>h</sup> Centre for Research and Graduate Studies, University of Cyberjaya, Persiaran Bestari, 63000 Cyberjaya, Selangor, Malaysia

<sup>i</sup> School of Chemical Engineering, Yeungnam University, Gyeongsan 38541, Republic of Korea

<sup>j</sup> Department of Chemical Engineering and Materials Science, Yuan Ze University, Taoyuan, Taiwan

## ARTICLE INFO

### Keywords:

Duckweed  
Pre-treatment  
Nano-composite  
Total reducing sugars  
Microbial community

## ABSTRACT

The incredible growth of the duckweed (DW) in the water ecosystem causes severe environmental problems and reduces biodiversity. Harvesting and valorization of such plants represents a challenge due to its richness with organics. Hydrogen productivity (HP) from dark fermentation of delignified duckweed (DDW) is the main objective of current research. The anaerobes cultures were immobilized on the Graphene/hydroxyapatite nano-composite (nG/HAP) for enhancement of hydrogen yield (HY) and enzymes activities. The HP of  $13.5 \pm 0.78$  mL was obtained from the fermentation of native DW and significantly increased up to  $208.9 \pm 12.6$  mL for delignified one. This was linked to an increase of the hydrogenase enzyme (HE) activities from  $0.02 \pm 0.0003$  to  $0.109 \pm 0.004$  mg M.B reduced/min. The HP was further increased up to  $387.1 \pm 13.6$  mL for batches containing 80 mg/gVS of nG/HAP. nG/HAP inhibited the competitors and promoted the cooperators for the *Firmicutes* hydrogen producers.

## 1. Introduction

Duckweed plants (*Lemna gibba*) lives in polluted water streams [1]. The plants excessively grow resulting in high biomass rich nutrients due to the uptake of contaminants from water [2]. Nowadays, these plants are utilized for the removal of heavy metals [3], 1,4 dioxane [4], nutrients [5] and pharmaceuticals [6,7] from wastewater industry. The presence of the DW in the water streams causes several environmental problems i.e. minimization of the sunlight penetration [8], shelter for unwanted animals and depletion of oxygen [9]. Harvested such plants with a high biomass yield of  $23.87\text{--}36.17\text{ g/m}^2\text{d}$  from water streams are necessary to keep the clean ecosystem and biodiversity [10].

Fortunately, the dry biomass of DW plants is composed of carbohydrate (17.6–35 %), starch (21–38 %), crude protein (16–41.7 %), crude fiber (8.8–15.6 %) and lipids (4.5–9 %) [11]. Hence, the DW biomass is suitable for bioenergy productivity via anaerobic digestion process [12–16]. The DW was earlier attempted for production of bioethanol (Et-OH) [17], biochar [18] and biogas [19]. Delignification of the DW prior anaerobic digestion (AD) process is necessary to break down the lignin layer and converts the hemicellulose fractions into easily biodegradable sugars [20–22]. Acid hydrolysis (1 %  $\text{H}_2\text{SO}_4$ ) of DW prior fermentation process provided maximum HP of 169.30 mL/g dry weight at  $35^\circ\text{C}$  and initial pH value of 7.0 [23]. Thermal – acid pretreatment (1 %  $\text{H}_2\text{SO}_4$ ,  $T = 85^\circ\text{C}$  for 1 h) of DW resulted HY of 75 mL/g dry DW within 7 days and H<sub>2</sub> content was 42 % [24]. The delignification of DW

\* Corresponding authors at: College of Materials and Chemical Engineering, Heilongjiang Institute of Technology, Harbin 150050, People's Republic of China (X. Tan); Department of Chemical Engineering and Materials Science, Yuan Ze University, Taoyuan, Taiwan (K.S. Khoo).

E-mail addresses: [prof.tawfik.nrc@gmail.com](mailto:prof.tawfik.nrc@gmail.com) (A. Tawfik), [tanxuefei2016@126.com](mailto:tanxuefei2016@126.com) (X. Tan), [msakhtar@ynu.ac.kr](mailto:msakhtar@ynu.ac.kr) (M.S. Akhtar), [kuanshiong.khoo@hotmail.com](mailto:kuanshiong.khoo@hotmail.com) (K.S. Khoo).

Abbreviations	
DW	Duckweed
HP	Hydrogen productivity
HPR	Hydrogen production rate
DDW	Delignified duckweed
CODt	COD total
CODs	COD soluble
COD p	COD particulate
TS	Total solids
vS	Volatile solids
S	Sludge
NPs	Nanoparticles
nG/HAP	Graphene/hydroxyapatite nano-composite
qPCR	Quantitative PCR
OTUs	Operational Taxonomic Units
GO	Graphene oxide
nG	Graphene nanoparticles
HFo	Formate
HPr	Propionate
iso-HBu	Iso-butyrate
HVa	Valerate
HAc	Acetate
VFAs	Volatile fatty acids
TPC	Total phenolic content
HE	Hydrogenase enzyme
EDX	Energy dispersive X-ray
SEM	Scanning electron microscopy
TEM	Transmission electron microscope
FTIR	Fourier-transform infrared spectroscopy
XRD	X-ray diffraction
EPS	Extracellular polymeric substances
XPS	X-ray photoelectron spectroscopy
HY	Hydrogen yield

plants accelerates the activities of the enzymes of anaerobes; enhances the hydrolysis process and subsequently bioenergy yield [25–28]. However, the yield of phenolic compounds in the hydrolysate of DW highly reduces the metabolites activities and bioenergy productivity [29,30]. Little attention has been paid to HP from delignified duckweed (DDW) due to low bioenergy productivity and not being economically feasible. In this investigation, enhancement of HP and yield from DDW by anaerobes immobilized on nanoparticles was extensively investigated [31–34].

Several attempts have been tried to increase the HP and HY from low-cost substrates by immobilization of anaerobes on nanoparticles (NPs) [21]. The addition of NPs increased the HE activities, electron transphere by anaerobes and NADH/NAD<sup>+</sup> ratio [35]. Further, the NPs cause a shift from microbial butyrate to the acetate pathway. This will supply more NADH, in the fermentation medium that can serve as an electron carrier for H<sub>2</sub> formation (Eq. (1)). The dehydrogenase and hydrogenase enzymes activities were increased from 0.216 to 0.301 mL/gVSS.min and from 13.92 to 20.36 mg/gVSS.min respectively with the addition of Fe<sub>3</sub>O<sub>4</sub>NPs [36]. Ag-NPs increased the number of *Methanosarcina* genus by 5-fold compared to the control samples indicating the positive impact of addition of NPs on the microbial growth and activities [37]. The electric unique conductive nature of NPs promotes bioenergy generation by transfer of electrons between fermentative bacteria and acidogenesis/methanogen [38].



The HY from fermentation of black liquor in the presence of magnetite nanoparticles was increased up to 1.41 ± 0.13 mol/mol glucose due to an enhancement of xylanase, polygalacturinase and protease enzymes activities [20]. Elreedy et al., [39] found that anaerobes supplemented with NPs of 200 mg α-Fe<sub>2</sub>O<sub>3</sub>/L, 20 mg NiO/L and 10 mg ZnO/L significantly increased HY from mono-ethylene glycol rich wastewater by 41, 30, and 29 % respectively. Further improvement of HY was occurred with the immobilization of anaerobes on dual and multi-NPs due to the increase of *Clostridiales* (*Clostridiaceae family* > 83 %) in the fermentation medium [40]. Hematite NPs increased the hydrogen production rate (HPR) from 3.87 to 5.9 L/L.d during fermentation of sucrose wastewater [41]. Mixed culture bacteria supplied with NPs of 100 mg/L magnetite/graphene oxide and fed with gelatinous wastewater industry promoted HY up to 112.4 mLH<sub>2</sub>/gCOD removed. This was due to a high biodegradation efficiency of 80.8 % for carbohydrates, 34.4 % for proteins and 31.4 % for lipids. *Proteobacteria*, *Firmicutes*, *Clostridia* and *Bacilli* activities were dominant for conversion of gelatinous wastewater industry [42]. The toxicity of phenolic compounds were highly reduced from 455 ± 22.5 to 135 ± 12.7 µg Gallic

acid equivalent/mL in the presence of Graphene NPs which facilitate the electron transfer between the microorganism and substrate [43]. Fe<sub>3</sub>O<sub>4</sub> and Ni NPs accelerated the *Azolla microphylla* degradation rate by 89.8 % and bioenergy yield by 49.1 % due to direct interspecies electron transfer (DIET) [44].

To the best of author's knowledge, the nG/HAP was studied for the removal of methylene blue dye from wastewater [45], NiFe<sub>2</sub>O<sub>4</sub>/hydroxyapatite/Graphene for removal of cadmium from wastewater [46], biomedical applications [47], the capture of strontium [48], photocatalyst and adsorption of Pb<sup>2+</sup> ions [49,50]. However, the impact of the addition of nG/HAP on the hydrogen-producing bacteria (HPB) from DDW is yet discussed except the study of [21]. Therefore, the current objective of the present work is to investigate the impact of the immobilization of anaerobes on nG/HAP for 1. hydrogen productivity 2. phenolic compounds removal 3. hydrolytic enzymatic activities 4. carbohydrates and proteins degradation, and extracellular polymeric substances (EPS) secretion during dark fermentation of delignified duckweed. Meanwhile, the high throughput 16S rRNA sequencing was conducted to confirm bacterial community shift induced by nG/HAP. The correlations between the community members were identified to further explore the effect of bacterial responses to nG/HAP on the overall hydrogen productivity by the anaerobes.

## 2. Materials and methods

### 2.1. Thermal pretreatment assisted alkalization of duckweed plants

The DW was harvested from water streams situated in the Giza governorate (Egypt). The composition of DW biomass in terms of cellulose, lignin, hemicellulose, protein, carbohydrate and ash content are presented in Table 1. The plants were dried in the oven at a temperature of 100 °C for 24 h. Thermal pretreatment assisted alkalization process was used for delignification of DW. 200 g DW was delignified by 1.75 % NaOH (w/v) at a pressure of 1.5 bars and 180 °C for 2 h., in stainless steel autoclave. The delignified duckweed (DDW) was brownish with a pH value of 12.75 which was carefully neutralized to be 7.5 by phosphoric acid to enrich the substrate with nutrients necessary for anaerobic digestion process. The DDW contained suspended fibers in the bulk liquid. The valerate (HVa), propionate (HPr), iso-butyrate (iso-HBu), formic (HFa) and acetate (HAc) in the DDW was accounted for 123.4 ± 12.8 mg/L, 122 ± 8.9 mg/L, 244 ± 17.6 mg/L, 180 ± 10.8 mg/L and 223 ± 17.1 mg/L respectively (Table 1). Total reducing sugars (TRS) of 1467.9 ± 13.2 mg/L and total phenolic compounds (TPC) of 1710.8 ± 22.6 mg/L was recorded in the DDW due to the alkalization process. The carbohydrate was quite high and amounted to 34.9 ± 2.8 g/L which is

**Table 1**

Characteristics of the native, delignified duck weed (DDW) and inoculum sludge.

Parameters	Duck weed (DW)	Delignified duck weed (DDW)	Inoculum sludge
pH	–	7.5	6.7
Cellulose (%)	46.61 ± 0.53 (%)	34.3 ± 0.8 (%)	–
Hemicellulose (%)	36.9 ± 0.2 (%)	12.8 ± 0.06 (%)	–
Lignin (%)	11.3 ± 0.38 (%)	3.1 ± 0.03 (%)	–
Ash content (%)	5.2 ± 0.3 (%)	4.1 ± 0.2 (%)	–
Valerate (HVa) – mg/L	–	123.4 ± 12.8	12.6 ± 0.2
Propionate (HPr) – mg/L	–	122 ± 8.9	22.3 ± 0.9
Iso-butyrate (iso-HBu) – mg/L	–	244 ± 17.6	33.2 ± 1.6
Format (HFa) – mg/L	–	180 ± 10.8	3.9 ± 0.2
Acetate (HAc) – mg/L	–	223 ± 17.1	32.8 ± 3.2
Total reducing sugars (TRS) – mg/L	–	1467.9 ± 13.2	–
Total phenolic compounds (TPC) – mg/L	–	1710.8 ± 22.6	–
Carbohydrate – g/L	37.8 ± 2.3 (%)	34.9 ± 2.8	–
Protein – g/L	22.9 ± 1.7 (%)	6.8 ± 0.78	–
COD total – g/L	–	35.3 ± 2.3	34.1 ± 7.3
COD soluble – g/L	–	34.6	2.6 ± 0.3
Volatile solids (VS) – g/L	–	44.1 ± 2.4	48.75 ± 0.35
Total solids (TS) – g/L	–	65.9 ± 4.4	76.04 ± 0.34
α-amylase – U/100 mL	–	–	8.7.0 ± 0.4
Xylanase – U/100 mL	–	–	8.0 ± 7.8
CM-cellulase – U/100 mL	–	–	3 ± 1.2

essential for biodegradation and metabolism process. The protein was quantified to be  $6.8 \pm 0.78$  g/L. The soluble COD represented 98 % of the total COD and the particulate fraction was quite low (2.0 %) indicating the solubilization of the DW. The COD and volatile solids (VS) were  $35.3 \pm 2.3$  and  $44.1 \pm 2.4$  g/L in the DDW respectively.

## 2.2. Mixed culture anaerobes

The anaerobes were sampled from an anaerobic digester (Al-Gabal Al-Asfer-Egypt). The settleability of the harvested inoculum sludge was 37.8 mL/gTS. The contents of TS and VS were  $76.04 \pm 0.34$  and  $48.75 \pm 0.35$  g/L (Table 1). The VS/TS ratio of the inoculum sludge was 0.64. The mixed cultures were daily supplemented with DDW for an acclimatization period of a month to enrich the inoculum with hydrogen producers avoiding thermal pretreatment process. Likely, the highest HY of 75.3 mL/gvS was obtained from fermentation of food waste using untreated inoculum anaerobic sludge [51]. Anaerobic sludge was directly used for HY of 126.5 mL/gVS.d from food waste without pretreatment of inoculum for a period of 48 days [23]. The CODs was quite low in the inoculum sludge and represents 7.6 % of the CODtotal. The CODp/CODt ratio was 92.4. α-amylase-, xylanase, CM-cellulase was  $8.7.0 \pm 0.4$ ,  $8.0 \pm 7.8$  and  $3 \pm 1.2$  U/100 mL, respectively.

## 2.3. Graphene/hydroxyapatite nano-composite

The nG/HAP was synthesized by hydrothermal method. 600 mg of Graphene oxide nanoparticles (nGO), 4.8 mM  $(\text{NH}_4)_2(\text{HPO}_4)$  and 8 mM of  $\text{CaCl}_2$  with adjusting the pH value at a level of 10.0 using ammonium hydroxide ( $\text{NH}_4\text{OH}$ ) [21]. The mixture was heated in a stainless-steel Teflon lined autoclave at  $180^\circ\text{C}$  for 24 h. The composite was regularly washed with deionized water and ethanol, centrifuged and dried at  $70^\circ\text{C}$  for 24 h [52].

## 3. Experimental procedures

Triplicate anaerobic batch assays experiments were conducted in serum bottles as shown in Fig. 1. The batches with a volumetric capacity of 250 mL were used. 200 mL is the working volume of each serum bottle. The 1st bottles set were supplied with 100 mL sludge (S) ( $48.75 \pm 0.35$  gVS/L), 20.0 g duckweed and 80 mL dist. water. These bottles

were used as a control to assess the gas production from the native duckweed plants. The 2nd bottles set were supplemented with 100 mL sludge (S) ( $48.75 \pm 0.35$  gVS/L) and 100 mL DDW ( $35.3 \pm 2.3$  gCOD/L) resulting in food to microorganism (F/M) ratio of 0.36 gCODt/gVS in the fermentation medium. (F/M) ratio was calculated from the following Eq. (2). All experimental runs tests were examined at constant F/M ratio of 0.36 gCODt/gVS to mitigate the toxicity of total phenolic compounds (TPC) and maximize the HP at optimum nG/HAP dosage. The maximum  $\text{H}_2$  production rate ( $R_m$ ) of 17.979 mL  $\text{H}_2$ /h was obtained from palm oil mill waste rich TPC at F/M ratio of 0.4 gCOD/gVS [53].

$$\frac{F}{M} \text{ ratio} = \frac{\text{COD(g)}_{DDW} \times \text{Samplevolume(L)}}{\text{VS(g)}_{DDW} \times \text{Workingvolumeofbottle(L)}} \quad (2)$$

The main experimental bottles sets (100 mL (S) + 100 mL (DDW) were supplemented with 10, 30, 40, 60, 80 and 120 mg/gVS (nG/HAP). The pH value of all bottles set was adjusted at a pH level of 7.5 using phosphoric acid to be utilized as a nutrient source and suitable for growing of the anaerobes cultures. The initial fermentation pH value was 7.5 avoiding a sudden drop due to the volatile fatty acids (VFAs) productivity and accumulation. The initial pH was progressively dropped from 7.5 to  $5.8 \pm 0.2$  after fermentation period of 14 days. The  $\text{H}_2$  content of 46–55 % remained unaffected at initial pHs (5.5–8.5) of fermentation thermal-acidified DW [24]. The hydrogen potential of 70.19 mL and maximum  $\text{H}_2$  production rate of 12.43 mL  $\text{H}_2$ /L was obtained from fermentation of banana waste at temperature of  $37^\circ\text{C}$  and pH value of 7.0 [54]. The batches had a headspace of 50 mL to allow the gas production. The bottles were flushed for 3.0 min using nitrogen gas to sustain anaerobic environmental conditions in the fermentation reaction medium. The bottles set were incubated at  $35 \pm 0.2^\circ\text{C}$  for a period of 350 h. The maximum HP from pre-treated DW was obtained by Mu et al., [55] at temperature of  $35^\circ\text{C}$ .

The volumetric biogas productivity was daily measured by displacement method. The biogas composition in terms of  $\text{H}_2$ ,  $\text{CH}_4$  and  $\text{CO}_2$  was daily measured. The  $\text{H}_2$  potential (P – mL), maximum  $\text{H}_2$  production rate ( $R_{\max}$  – mL/h) was simulated based on the Gompertz equation model (Eq. (3)),

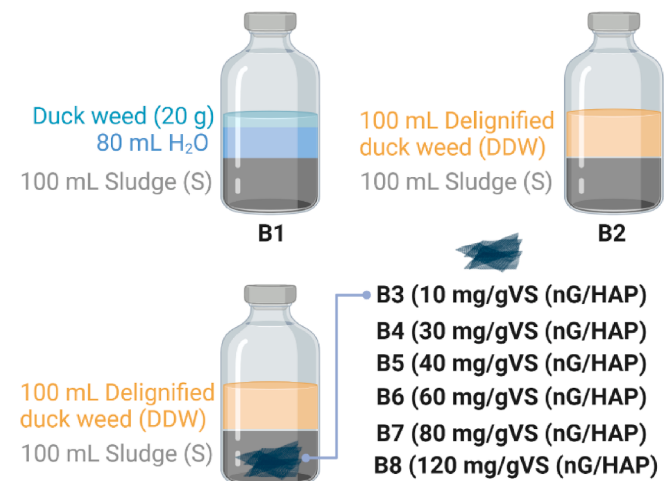


Fig. 1. Batch experimental set-up for hydrogen productivity from delignified duckweed (DDW).

$$B(t) = P^* \exp \left\{ - \exp \left( \frac{R_m^* e}{P} (\lambda - t) + 1 \right) \right\} \quad (3)$$

where B is the cumulative H<sub>2</sub> productivity (mL), t: is the fermentation time (h) and λ: is the lag phase duration (h).

### 3.1. Analytical methods

The Native DW, DDW, inoculum sludge (S) and nanoparticles (NPs) were analyzed. The lignin, cellulose, hemicellulose and ash content of the DW was analyzed based on the methods described by Soest et al., [56]. The pH was measured by JENWAY 3510. COD t, COD s, COD p, TS, and vS were determined based on APHA [57]. CODs were filtered using a 0.45 μm membrane filter and the COD p was calculated by subtracting CODt and filtered COD. Formate (HFo), propionate (HPr), acetate (HAc), iso-butyrate (HBu), valerate (HVa) were the main volatile fatty acids (VFAs) fractions and was determined by HPLC. Enzymatic assays of microbial carbohydrate-cleaving enzymes in terms of xylanase, polygalacturonase, α-amylase and CM-cellulase activities were measured based on the method of [58]. The total phenolic content (mg gallic acid equivalent (GAE)/ mL) of the samples was measured based on the method described by Velioglu et al. [59]. Dubois et al. [60] method was used for the determination of carbohydrates. Hydrogenase enzyme (HE) activity was determined by the methylene blue reduction method [61]. Protein content was determined by the method of Emami Bistgani et al., [62]. Gas chromatography (GC-2014, Shimadzu, Japan) with helium as the carrier gas at a flow rate of 25 mL/min. was used for measurement of biogas composition. Energy dispersive X-ray (EDX) and Scanning electron microscopy (SEM) was used to observe the morphology of the nG /HAP and elemental analysis content. Transmission electron microscope (TEM), Model JEM-2010, Japan, was used to investigate particle size of NG /HAP. The main elements of nG/HAP were determined by Fourier-transform infrared spectroscopy (FTIR) in the range of 4000 to 450 cm<sup>-1</sup> (JASCO 6100 spectrometer, Japan). X-ray diffraction (Schimadzu XRD 7000, Japan) was used for the characterization of the nG/HAP.

### 3.2. Microbial analysis community

DNA extraction was conducted for the selected batches of 80 mg nG/HAP/gVS (N1), 120 mg nG/HAP/gVS (N2), 60 mg nG/HAP/gVS (N3), and control sample (N4). Quantitative PCR (qPCR) was carried out for the bacterial communities and archaeal of the samples targeting the 16S rRNA gene. The samples were analyzed in triplicates. DNA standards were used to estimate gene copy numbers. Single-Strand Conformation Polymorphism of the microbial community was conducted based on [63]. ABI 310 Genetic Analyzer was used to carry out the Capillary-Electrophoresis-SSCP process [63]. Statistical analysis and Operational Taxonomic Units (OTUs) assignments were conducted as previously described by Poirier et al., [64]. The sequences were analyzed by Quantitative Insights into Microbial Ecology software [65]. Three amplicons USEARCH v5.2.136 [66], MOTHUR v.1.25.0 [67], and QIIME 1.8.0 [65] read processing pipelines were carefully checked for the quality of the reads. Sequences shorter than 180 bp and low quality score (<20) were unaccounted. Chimeric sequences were removed and sequences were clustered into OTUs with 97 % sequence similarity using quality filter (USEARCH) (<https://www.drive5.com/usearch/>) reference set [68]. Qualified sequences were clustered into OTUs specified by a 3 % distance level based on the distance matrix and a bootstrap higher than 60 %. The Ribosomal Database Project classifier was assigned to the corresponding taxa. The rarefied OTU table by the package ‘vegan’ in R was used to calculate the Shannon indices, ACE, Simpson and Chao1 [69]. Confidence values (<80 %) (phylum level) were unclassified according to Wang et al., [70].

## 4. Results and discussion

### 4.1. Characterization of Graphene /hydroxyapatite nano-composite

Graphene and hydroxyapatite (HAP) are known for their high biological biocompatibility, superior mechanical, electrical and thermal conductivity properties [71]. Fig. 2 shows SEM (a), TEM (b), EDX (c), XRD (d) and FTIR spectra (e) of nG/HAP. The morphological shape of the nG/HAP was examined by the SEM images (Fig. 2a) giving high agglomeration of nano-composite materials. The Graphene has appeared fluffy appearance combined with a high agglomeration of HAP sheets. The original structure of Graphene was not changed but its surface roughness is increased [71]. The particle size depends on the nucleation between HAP and Graphene molecules [52]. The aggregations and crystallization of nHAP were detected by TEM imaging (20 nm diameter and 30–50 nm length nano-rods) (Fig. 2b). The signals of Ca and P were successfully detected indicating that the rod-like HAP which clearly grew onto the Graphene surface [71]. The diffraction of nG/HAP showed polycrystalline diffraction rings. The starting molar ratio of 1.9 for calcium (Ca) and phosphorus (P) was confirmed by the EDX results as shown in Fig. 2c. The carbon (C) of 30.28 W%, oxygen (O) of 35.02 W%, P of 11.94 W% and Ca of 22.75 W% is presented in Fig. 2c. The Ca content of 10.54 at.% and P concentration of 8.12 at.% was observed for HAP by X-ray photoelectron spectroscopy (XPS) indicating the existence of hydroxyapatite [71].

The X-ray diffraction (XRD) pattern shows signals at 2θ of 25.88°, 31.88°, 32.28°, 34.08°, 39.78° and 49.58°, corresponding to the diffraction planes (002), (211), (112), (202), (130) and (213), respectively indicating the presence of nHAP (JCPDS no. 01-073-8417) (Fig. 2d). The diffraction peak (002) was appeared in nG/HAP, confirming the successfully graphite exfoliation [71]. The XRD results confirmed the formation of nHAP. These signals assure the deposition of nHAP in a hexagonal structure. Likely, Li et al., [71] detected diffraction peaks of 25.9°, 31.8°, 32.1°, 34.18°, 39.6°, 46.6°, 49.4° and 53.34° due to (002), (211), (300), (202), (130), (222), (213), and (004) planes of HAP. The broad X-ray diffraction peaks centered at approximately 2θ of 19° was for Graphene which corresponds to the (002) reflection.

FTIR spectrum showed characteristic absorption peaks of nG/HAP nano-composite as shown in Fig. 2e. The broad bands observed at 3430 cm<sup>-1</sup> with high intensity are mainly arisen from the O—H group stretching vibrations. Fang et al., [72] found that O—H/N—H stretching vibration of nG/HAP was observed at 3600–3100 cm<sup>-1</sup> due to the presence of O—H bonds of HAP and water molecules. The low intensity peaks at 2930 cm<sup>-1</sup> and 2840 cm<sup>-1</sup> appeared due to sp<sup>2</sup> and sp<sup>3</sup> stretching C—H bands. The peak at 1633 cm<sup>-1</sup> arises from stretching of C—C aromatic and the highest intensity peak at 1047 cm<sup>-1</sup> corresponds to the C—OH stretching. Those peaks was appeared due to a reduction of Graphene oxide (GO) onto Graphene. Bands detected at 589 and 1048 cm<sup>-1</sup> are characteristic for PO<sub>4</sub><sup>3-</sup> group. The band for P—O stretching was observed at 589 cm<sup>-1</sup>. Likely, the hydroxyapatite were detected at peaks of PO<sub>4</sub><sup>3-</sup> at 605, 1035 and 566 cm<sup>-1</sup> [71]. The PO<sub>4</sub><sup>3-</sup> and OH groups bands of HAP were observed by Hendi and Yakuphanoglu [52] at 960–963 cm<sup>-1</sup> and 561–602 cm<sup>-1</sup> respectively.

### 4.2. Effect of Graphene/hydroxyapatite nano-composite dosage on hydrogen productivity and yield from delignified duckweed

nG/HAP is rich in Ca which is necessary for bacterial growth degrading wastes [21]. The Graphene is responsible for electron transfer from bacteria to hydrogen producers for enhancement of enzymes activities [43]. However, the HP and HY are mainly dependent on the nG/HAP concentration. Fig. 3a shows the effect of nG/HAP dose on HP. The HP of 13.5 ± 0.78 mL was harvested from dark fermentation of native DW where the hydrogenase enzymes (HE) activities were quite low and amounted to 0.02 ± 0.0003 mg M.B reduced/min. Further, the

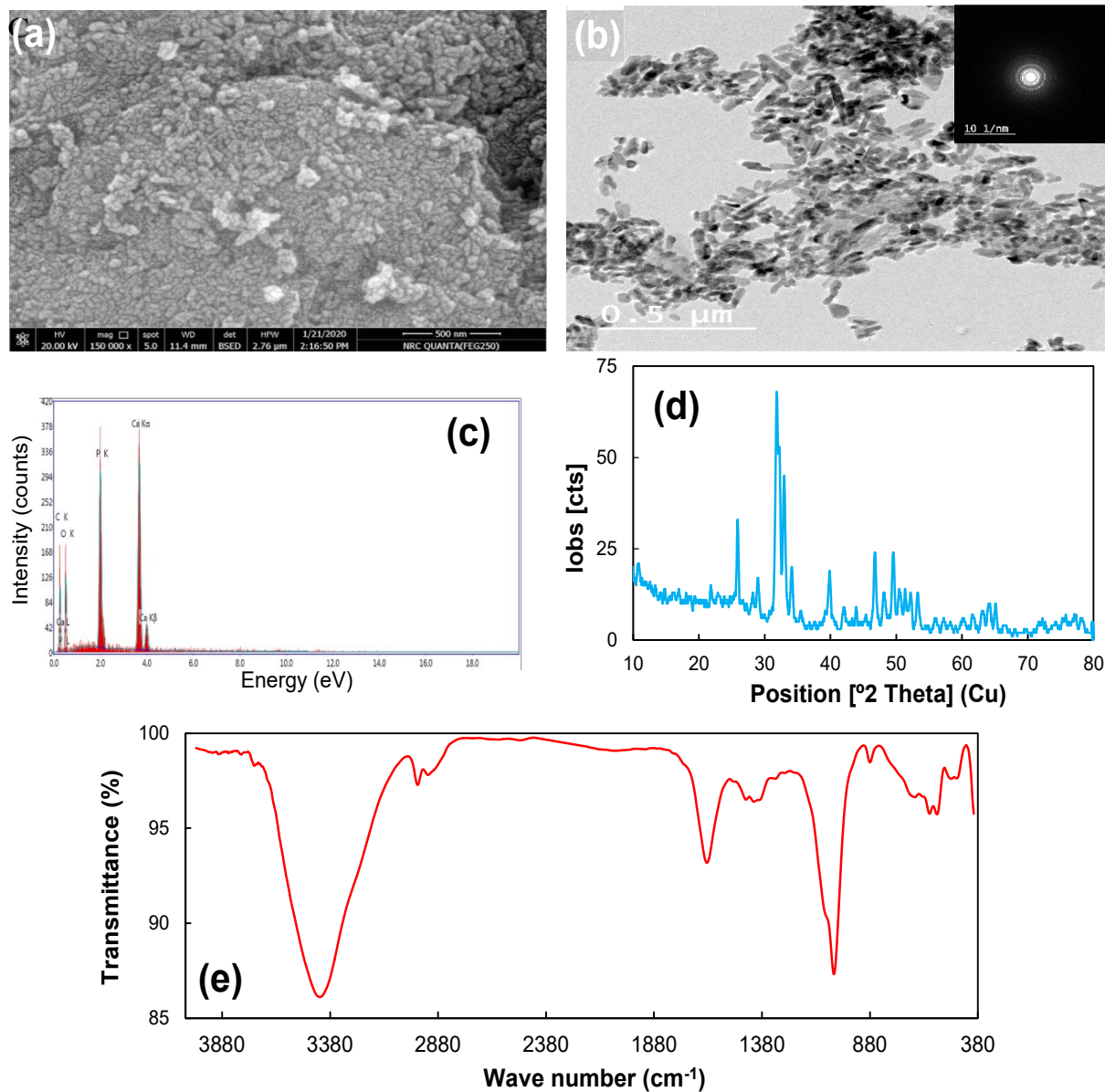


**Fig. 2.** SEM (a) TEM + diffraction (D) (b), EDX (c) XRD (d) and FTIR spectra (e) of Graphene /hydroxyapatite nano-composite (nG/HAP).

extracellular polymeric substances (EPS) were only  $78 \pm 6.7$  mg/gVS for dark fermentation of native DW. Native DW is lignocellulosic biomass containing lignin, hemicellulose and cellulose, which needs more contact time to break down into fatty acids and hydrogen by anaerobes (Table 1). The hydrolysis of those structure components is the rate-limiting step in anaerobic digestion process. Mixing of inoculum sludge with native DW facilitate to some extent the solubilization and hydrolysis of hemicellulose to produce hydrogen. The partial biodegradation of hemicellulose highly destabilizes the biomass recalcitrant structure allowing the HP [73]. The polysaccharides content in native DW amounted to 59 %, which utilized by acidogenesis for HP [55]. Those values of HP have significantly increased up to  $208.9 \pm 12.6$  mL for DDW plants. This is linked to the alkalization of DW breaking down the lignin layer and hemicellulose into reducing sugars which is necessary for HP. Theoretically, fermentation of 1 g-glucose produces hydrogen of 149.3 mL. Moreover, pre-treatment of the DW plants facilitate the accessibility of enzymes activities for the degradation process. The HE activities of  $0.09 \pm 0.001$  mg M.B reduced/min. and EPS of  $178 \pm 22$  mg/gVS was registered for the sample containing DDW sample. This increase was linked with the presence of total reducing

sugars (TRS) of  $1467.9 \pm 13.2$  mg/L in the pretreated feed stock (Table 1). However, the HP was still quite low compared with literature due to the release of TPC ( $1710.8 \pm 22.6$  mg/L) in the DDW. However, the HP was substantially increased from  $208.9 \pm 12.6$  mL to  $387.1 \pm 13.6$  mL with supply of 80 mg/gVS nG/HAP as shown in Fig. 3a. This is linked to an increase of the HE activities from  $0.109 \pm 0.004$  to  $0.288 \pm 0.02$  mg M.B reduced/min. (Fig. 3c). Moreover, increasing the nG/HAP dose from 10 to 80 mg/gVS augmented the EPS from  $212 \pm 22$  to  $322 \pm 21$  mg/gVS respectively (Fig. 3b). Nano-metals play a key role in the H<sub>2</sub> fermentative process i.e. Ca concentration of 50–150 mg/L improved HP and HY [74]. The presence of Graphene facilitates the electron transfer between the substrate and anaerobes. Moreover, it plays a crucial role as a carrier for anaerobes creating unusual conditions for hydrogen-producing bacteria (HPB). The surface area of Graphene is quite high to facilitate the electrons adsorption and subsequently electron transfer between nG and HE molecules to catalyze the conversion of H<sub>2</sub> to proton and vice versa. Moreover, the addition of nG increased the enzymatic activities degrading proteins and carbohydrates i.e. xylanase, α-amylase, protease and CM-cellulase. The addition of hydroxyapatite rich calcium onto the anaerobes will maintain a high cell density in the digester and

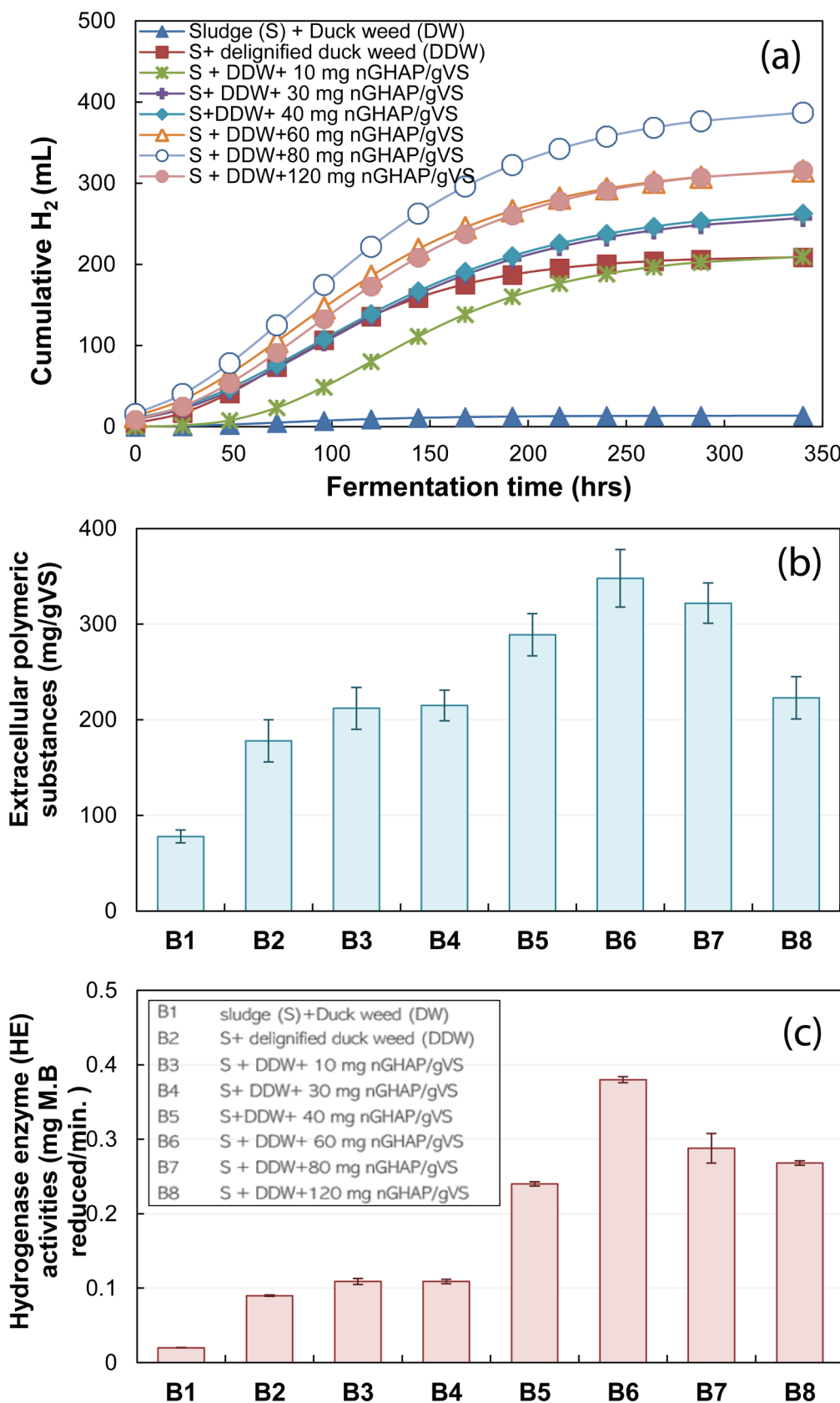


**Fig. 3.** (a) Modeled data for bio-H<sub>2</sub> productivity from dark fermentation of delignified duck weed based on modified Gompertz equation, (b) effect of Graphene/hydroxyapatite nano-composite (nG/HAP) dosage on extracellular polymeric substances and (c) hydrogenase enzyme activities.

induce microbial aggregation [75]. Moreover, Ca would improve the granulation process by facilitating early aggregation resulting in large particle sizes and more biomass growth [74]. The hydroxyapatite rich Ca would enhance the secretion of EPS to keep the ionic balance in the reaction medium. Moreover, EPS are playing a key role in cell binding and agglomerating the anaerobes due to electrostatic interaction force. EPS is always negatively charged and can easily bind with positively charged organic pollutants and facilitate the metabolism process of the organic content of the DDW. EPS prefer to bind with divalent ions in the reaction medium to form more stable complexes [74]. The HP was dropped up to  $316.1 \pm 14.7$  mL at supplementation of 120 mg/gVS nG/HAP due to anaerobes dilution and increases osmotic pressure in the reaction medium. The experimental results were closely fitted to the simulated ones with  $R^2$  ranging from 0.975 to 0.995. The biogas composition content was almost remained unaffected for all batches and amounted to 51–56 % for  $H_2$ , 13–17 % for  $CH_4$  and 20–26 % for  $CO_2$ . Some methanogenesis were detected in the batches due to the use of untreated inoculum sludge for fermentation of DW as shown in Fig. 6e.

The HY was only 1.35 L/kgDW for dark fermentation of the native DW which was increased up to 21.05 L/kgDW for hydrogenation of DDW. The DDW was further provided a high HY with supplementation of different doses of nG/HAP. The HY amounted to  $39.7 \pm 2.1$  and  $32.4 \pm 1.1$  L/kgDW for anaerobes supplemented with 80 and 120 mg/gVS of nG/HAP. These values were higher by values of 46 and 34 % as compared to batches supplied with 10 and 30 mg/gVS of nG/HAP respectively. Likely, immobilization of anaerobes on  $Fe_2O_3$  NPs improved HY by 57.8 % from the wastewater industry [76]. HY was increased by 26.4 % by anaerobic sludge supplemented with  $Fe_3O_4$  NPs (400 mg/L) under mesophilic conditions [77]. 50 mg/L of  $Fe_3O_4$  NPs was sufficient to improve the HY by a value of 83.3 % (44.3 L/kg COD) using mixed culture from distillery wastewater [78]. Mostafa et al., [42] found that immobilization of anaerobes on 100 mg/L magnetite/Graphene oxide increased the HY up to 112.4 mL $H_2$ /gCOD removed from gelatinous wastewater and the conversion efficiency of proteins, carbohydrates and lipids were promoted up to 34.4, 80.8 and 31.4 %, respectively.  $H_2$  productivity was significantly increased by 1.5 times with anaerobes supplemented with nickel oxide and hematite NP resulting in an increase of HY by a value of 32.6 % [79]. Yuan et al., [80] found that supplementation of 100 mg/L Ca improved the cell retention, density by twofold, HY and HPR of 3.74 mol  $H_2$ /mol sucrose and 24.5 L/dL, respectively. Calcium ion addition of 75–150 mg/L enhanced the granulation process and increased HY up to 3.6 mol  $H_2$ /mol-sucrose and HPR of 807 mmol- $H_2$ /L-d. However, the HPR and HY were deteriorated at a Ca concentration of 300 mg/L [74]. The lag phase period was largely reduced from 20 h, for the control sample to 12.0 h, for anaerobes immobilized on nG/HAP. This indicates that the addition of nanoparticles rich calcium accelerated the biodegradation activities and subsequently hydrogen productivity. Likewise, the HY was increased by 27 % due to the co-addition of NPs (50 mg/L  $Fe_2O_3$  + 10 mg/L NiO) as compared with controls and a significant decrease of the lag phase from 3.6 to 2.8 h was occurred [81]. The HP of 150 L/kg vS was maximized at Ni and Fe concentration of 37.5 mg/L and the HY was improved by 200 % as compared to controls [82].

#### 4.3. Effect of Graphene/hydroxyapatite nano-composite dosage on the total phenolic compounds, total reducing sugars degradations, enzymatic carbohydrate and protein -cleaving

Bacterial cells are unable to up-take the macro-molecules i.e. carbohydrates and proteins present in native DW. Therefore, anaerobes produce extracellular hydrolytic enzymes such as  $\alpha$ -amylases, cellulases and proteases to solubilize the macromolecular into sugars and amino acids to facilitate the transport of substrate into the cell membrane [83]. Those simple by-products are utilized by anaerobes to have energy and synthesize new cellular cells. Polysaccharides (cellulose) are converted into simple sugars by the cellulase enzyme to produce glucose and the

starch is transformed into glucose by  $\alpha$ -amylase [84]. The hydrolysis process is normally a rate-limiting step for anaerobes degrading substrate containing high fractions of lignocellulosic matter. Fortunately, the major portions of organics in the DDW were in the soluble form (98 %). Understanding hydrolytic enzyme production, activities and its relations with nanoparticles supplementation are deeply discussed here. Fig. 4 shows the enzymatic activities of proteases, xylanase,  $\alpha$ -amylase, polygalacturonase and CM-cellulase for degradation of DDW.  $\alpha$ -amylase of  $4.8 \pm 0.02$  U/100 mL, xylanase  $5.9 \pm 0.008$  U/100 mL, CM-cellulase of  $10.9 \pm 0.9$  U/100 mL, polygalacturonase of  $4.8 \pm 0.008$  U/100 mL and protease of  $78 \pm 6.7$  U/100 mL was accounted for dark fermentation of native DW. Those values were significantly ( $P \leq 0.05$ ) increased up to  $22.3 \pm 2.2$ ,  $14 \pm 1.4$ ,  $5.9 \pm 0.9$ ,  $3.7 \pm 0.7$  and  $122 \pm 12.2$  U/100 mL for dark fermentation of DDW. The enzymatic hydrolysis was highly improved for delignified duckweed due to the breakdown of the lignin layer. Further improvement of the enzymatic activities occurred with supplementation of different concentrations of nG/HAP as shown in Fig. 4a and b. Morgan et al., [85] found that the addition of calcium onto the anaerobes promotes extracellular polysaccharide constituents which are utilized for cell bindings with the substrate.

The enzymatic activities of xylanase,  $\alpha$ -amylase, CM-cellulase, protease and polygalacturonase were  $67 \pm 6.7$ ,  $60 \pm 6$ ,  $78 \pm 7.8$ ,  $231 \pm 2.3$  and  $33.8 \pm 3.3$  U/100 mL for anaerobes supplied with 10 mg nG/HAP/gVS. Those values were increased up to  $188 \pm 18.1$ ,  $122 \pm 12.1$ ,  $178 \pm 17.2$ ,  $983 \pm 9$  and  $300 \pm 12.9$  U/100 mL for batches containing 80 mg/gVS of nG/HAP. This strongly indicates that the activities of the enzymes are promoted due to the supplementation of the anaerobes with nG/HAP. Amylase activity was quite high during the anaerobic digestion of potato waste due to the existence of amylolytic microbes [84].  $H_2$  production was increased by 60–70 % due to inoculation of the digester with hydrogen producer rich cellulolytic activities [86]. The addition of 20 g/L Zero valent iron increased the activities of protease and cellulase up to 92.0 and 91.7 %, respectively [87]. Hydrolytic enzymes caused a reduction of 80 % for total solids and 93 % removal of COD particulate [88]. The addition of  $\alpha$ -amylase (0.06 g/g dry sludge) increased the hydrolysis rate constant from 0.106 to 0.215 h<sup>-1</sup>. The activation energy for hydrolysis of volatile solids was reduced from 62.72 kJ/mol (control sample) to 20.19 kJ/mol ( $\alpha$ -amylase treatment) [89].

The anaerobes supplemented with nG/HAP provided a significant positive impact on the protein and carbohydrate degradation (Fig. 4a and b) as well as HY. The conversion efficiency of protein and carbohydrate was  $13.2 \pm 0.23$  and  $11.5 \pm 0.43$  % for dark fermentation of DW. These values were increased up to  $41.2 \pm 0.4$  and  $32.7 \pm 0.34$  % for fermentation of DDW. The addition of nG/HAP (80 mg/gVS) improved the degradation efficiency of protein ( $55.9 \pm 2.1$  %) and carbohydrates ( $39.5 \pm 1.3$  %). This can be attributed to higher protease,  $\alpha$ -amylase and xylanase activities. Likely, Feng et al., [87] found that the degradation efficiency of protein and carbohydrate was increased from 59.1 to 67.8 % and from 32.3 % to 43.4 % using anaerobes immobilized on zero-valent iron NPs. Similarly, the HY of  $15 \pm 0.05$  mL/g protein removed, and  $3.4 \pm 0.009$  mL/g carbohydrate removed was achieved by dark fermentation of DW. Delignification of duckweed provided higher HY of  $75.1 \pm 7.4$  mL/g protein removed and  $18.5 \pm 0.89$  mL/g carbohydrates removed. The HY was optimized at a level of  $104.4 \pm 8.3$  mL/g protein removed and  $28.8 \pm 0.034$  mL/g carbohydrate removed for the batches supplemented with 80 mg/gVS of nG/HAP.

The DDW contains total reducing sugars (TRS) of  $1467.9 \pm 33.2$  mg/L which are mainly glucose and fructose fractions. Those monosaccharides are further biodegraded by the acidogenesis process as shown in Fig. 4c and reported earlier by Zeng et al., [90]. The TRS removal was  $47.8 \pm 1.6$  % for the control batch containing only the DDW. The TRS removal was increased in the samples supplemented with nG/HAP. The TRS removal efficiency was maximized at levels of  $58.8 \pm 1.2$  and  $73.8 \pm 1.3$  % for the anaerobes supplemented with 10 and 80 mg/gVS of nG/HAP respectively. The removal efficiencies of TPC were  $17.5 \pm 1.6$  % for control batches and increased up to  $36.3 \pm 1.5$  % for

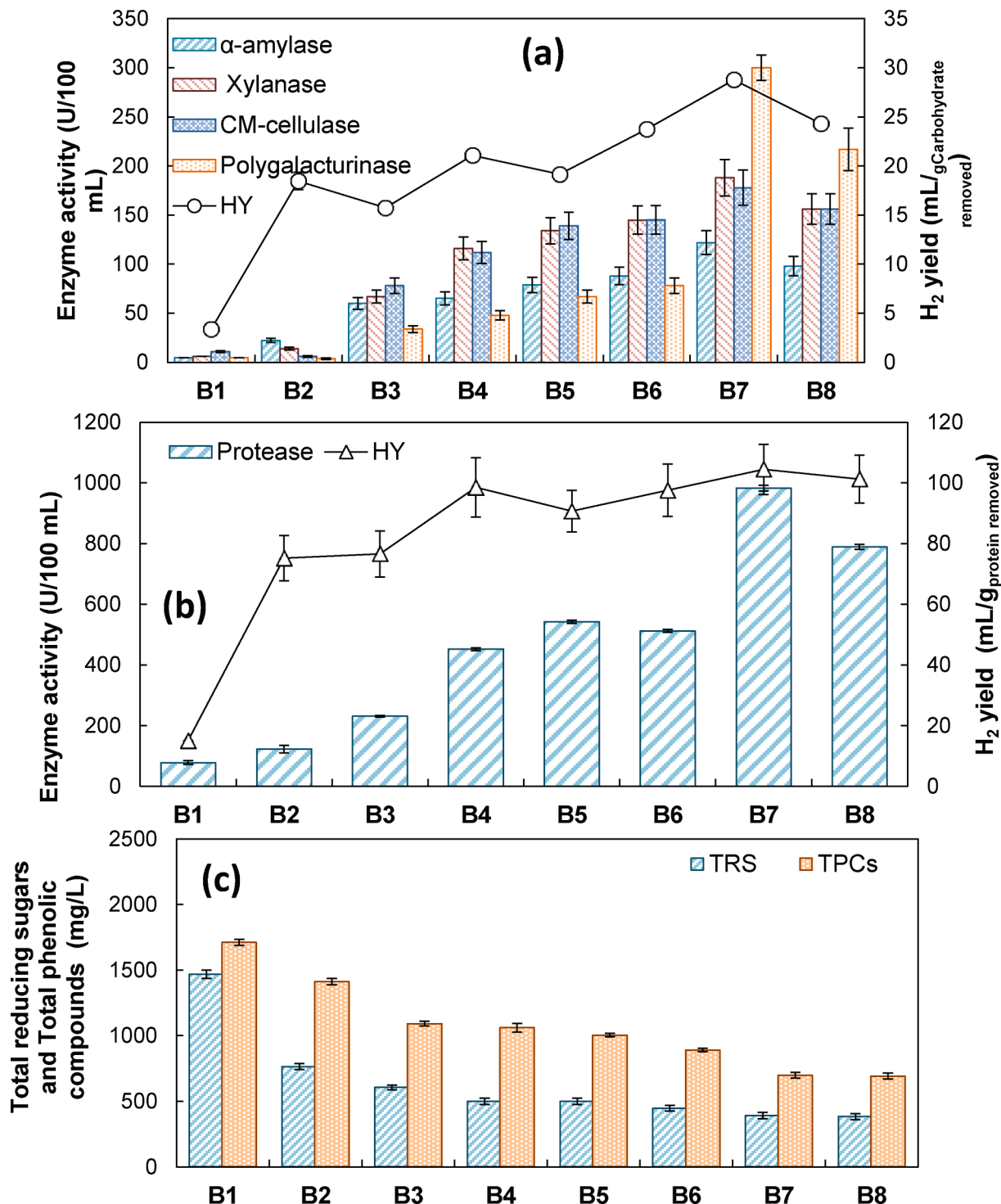


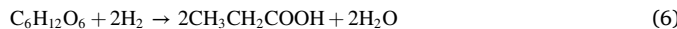
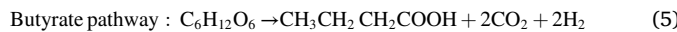
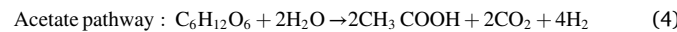
**Fig. 4.** (a) and (b) enzymatic activities for anaerobes degrading protein and carbohydrate, and (c) effect of nG/HAP dosage on the total phenolic compounds (TPC) and total reducing sugars (TRS) degradations.

the samples containing 10 mg/gVS of nG/HAP. Increasing the concentration of nG/HAP up to 80 mg/L increased the removal efficiency of TPC by 33.3 %. Likely, Hernandez and his coworkers [91] achieved the maximum biodegradation of phenolic compound of  $63.85 \pm 2.73\%$ , by anaerobes. However, the inhibition of methanization was occurred at high influent phenolic compounds of 800 and 1600 mg/L.

#### 4.4. Effect of graphene/hydroxyapatite nano-composite dosage on metabolite by-products

The acidogenesis process is employed for the biodegradation of amino acids and sugars into VFAs,  $H_2$  and  $NH_4-N$ . A drop in the pH values from  $7.5 \pm 0.2$  to  $5.8 \pm 0.2$  was occurred due to HAc, iso-HBu and HVa production in the fermentation medium. This can be attributed to the fixed amount of feed stock for all batches. Theoretically, conversion of organic matter into HAc and HBu produces 4.0 and 2.0

mol of H<sub>2</sub> respectively (Eqs. (4) and (5)). Production of HPr would utilize the H<sub>2</sub> gas (Eq. (6)) [92]. HAc to HBu ratio > 1 (Eq. (4)) and HAc/HBu < 1 (Eq. (5)) is the main acetate and butyrate fermentation pathway processes.



The results in Fig. 5 show the impact of supplementation of nG/HAP on the VFAs productivity in terms of HVa, HPr, iso-HBu, HAc and HFo in the fermentation medium. The iso-HBu, HPr, HFo and HAc was 190 ± 34.1, 122 ± 10.9, 244 ± 11.8, 180 ± 4.3 and 223 ± 12.7 mg/L and increased up to 320 ± 21.2, 365 ± 10 mg/L, 267 ± 12.9, 344 ± 10.9 and 298 ± 22.8 mg/L for fermentation of the DDW. The HBu pathway was dominant for dark fermentation of DW where the HAc/HBu ratio was 0.82 resulting HP of 208.9 ± 12.6 mL. The HVa, iso-HBu, HPr, HFo and HAc concentrations were increased in the fermentation medium by values of 58.0, 66.3, 44.7, 44.1 and 54.9 % in the batches supplemented with 10 mg/gVS of nG/HAP. Further improvement of HVa (68.9 %), iso-HBu (78.7 %), and HAc (81.4 %) productivity was achieved with supplementation of nG/HAP (80 mg/gVS) due to the shift of HBu into the HAc fermentation pathway at HAc/HBu ratio of 1.145. This behavior maximized the HP as shown in Fig. 3a.

The HY was 21.05 L/kgDW for hydrogenation of DDW and increased up to 39.7 ± 2.1 and 32.4 ± 1.1 L/kgDW for anaerobes supplemented with 80 and 120 mg/gVS of nG/HAP. This is linked with HPr accumulation in the fermentation medium at alkaline initial pH value of 7.5 (Fig. 5). The HPr was 267 ± 12.9 mg/L for batches containing DDW and dropped to 200 ± 10.3 and 144 ± 11.2 mg/L for batches containing 80 and 120 mg/gVS of nG/HAP. Apparently, initial pH value of 7.5 facilitates HPr accumulation rather than H<sub>2</sub> production. Moreover, HPr production pathways reduce powers that are potentially used for H<sub>2</sub> synthesis. Further, conversion of HPr into HAc could be occurred based on Eq. 6. The accumulation of HPr in the fermentation medium of DDW is explained by high levels of phenolic compounds (1710.8 ± 22.6 mgGAE/L) [93]. Poirier et al. [94] found that phenol concentration reduced the HPr oxidation rate due to hindering the microbial tolerance for levels exceeding 1.0 g/L.

#### 4.5. Bacterial $\alpha$ -diversity and community structure

A total number of 145,551 effective sequences were obtained for batch samples supplemented with 60 mg/gVS, 80 mg/gVS, 120 mg/gVS of nG/HAP and control sample. As shown in Fig. 6a-b, the batches

supplemented with 80 mg/gVS displayed the highest species richness compared to the other samples. The lowest ACE and Chao1 was obtained for batches containing DDW without nano-composite. Meanwhile, we observed higher species evenness in the batches supplied with 60 mg/gVS, 80 mg/gVS and 120 mg/gVS, as compared to the control batch sample based on the Simpson and Shannon indices (Fig. 6c-d). Such results indicated that the batches supplemented with 80 mg/gVS increased the biodiversity of the anaerobes where specific bacteria became dominant in the population and disappeared with the control sample. The previous study demonstrates that biodiversity acts as the insurance of community productivity [95] which may be the reason why anaerobes immobilized on 80 mg/gVS enjoyed the highest HY.

The results in Fig. 6e show the taxonomy of the samples harvested from batches of 60 mg/gVS, 80 mg/gVS, 120 mg/gVS and control sample to assess the variations of consortium and its relation with the HP and HY. Data displayed that all batch samples of 60 mg/gVS, 80 mg/gVS, 120 mg/gVS and control samples were dominated by the phyla i.e. Firmicutes (27.55 %), Proteobacteria (34.53 %), Actinobacteria (9.44 %), Bacteroidetes (3.82 %), Chloroflexi (10.19 %), and Planctomycetes (6.64 %). The abundances of Chloroflexi and Bacteroidetes were quite higher for the batch samples containing 80 and 120 mg/gVS of nG/HAP. However, no substantial difference was found in the common hydrogen producers, i.e., Firmicutes, particularly between the batches containing 80 mg/gVS of nG/HAP and control sample. The predominance of Firmicutes indicated its high tolerance to high phenolic compounds. This bacterial species have the capability for HP and HY at alkaline initial pH value of 7.5. However, abundance of Firmicutes, was decreased from 98.52 % at pH of 5 to 42.83 % at pH of 6.5 [23]. Moreover, the HPr accumulation < 344 mg/L has a minor effect on Firmicutes bacterial species as the H<sub>2</sub> content was kept at a level of 51–56 %. The order Clostridiales and Lactobacillales belongs to Firmicutes phyla which are enzymatic machinery efficient for biodegradation of polysaccharides and hydrolysis of lignocellulosic wastes [44]. Firmicutes was dominant bacterial phyla for HP from food waste [23]. Proteobacteria and Cyano-bacteria was < 8 and 6 % of the microbial community. The relative abundances of Proteobacteria and Actinobacteria were slightly lower in the anaerobes immobilized on 80 mg/gVS and 120 mg/gVS, than those the batches supplemented with 60 mg/gVS and control sample. The predominance of Actinobacteria was reported to be efficient for conversion of organic matters into organic acids [96]. This explained the reason for accumulation of VFAs in the batches supplemented with nG/HAP. The Archaeal community was detected at low levels in all batches particularly Euryarchaeota phyla producing a low quantity of methane (13–17 %).

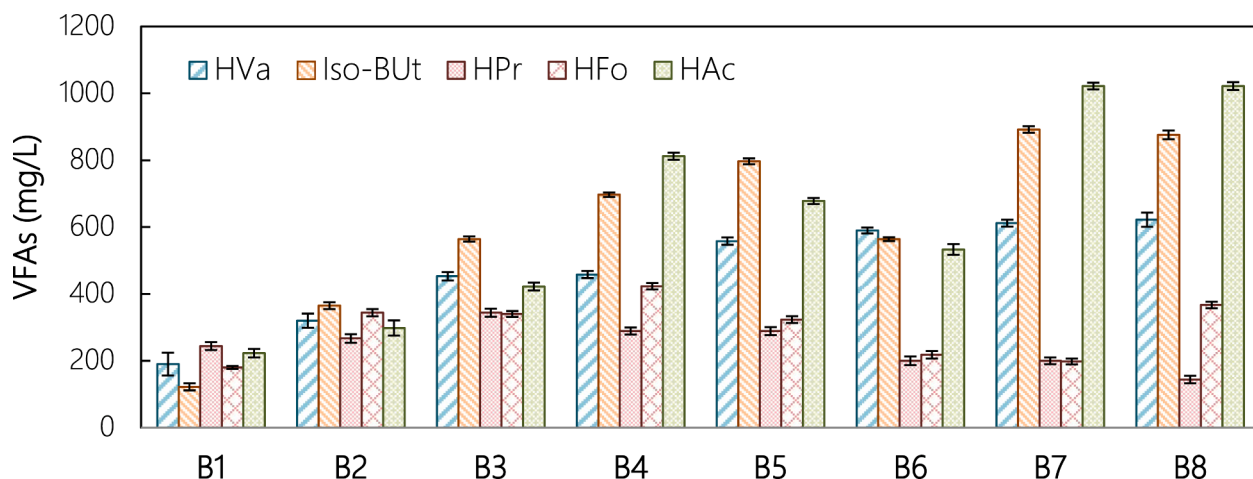
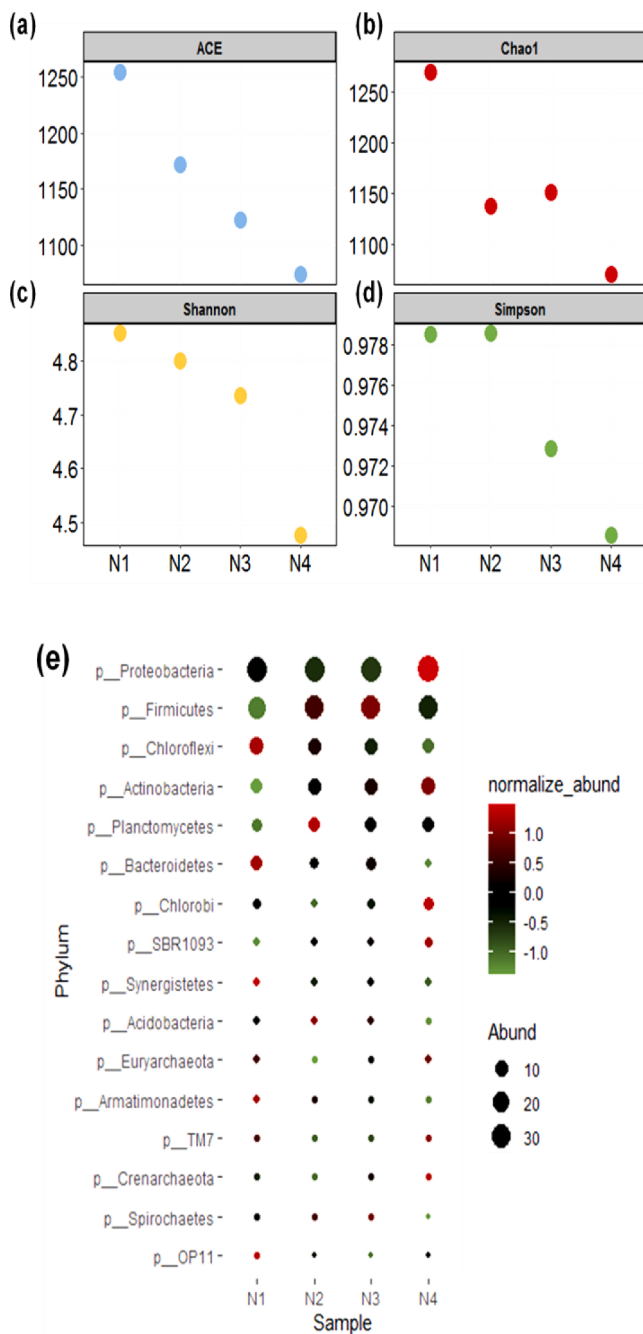


Fig. 5. Effect of Graphene/hydroxyapatite nano-composite (nG/HAP) dosage on metabolite by-products.



**Fig. 6.** Alpha-diversity and community structure of batches supplemented with 60 mg/gVS, 80 mg/gVS, 120 mg/gVS and control sample. The ACE (a) and Chao1 (b) indices are related to the absolute number of species in a given culture, while Simpson (c) and Shannon (d) indices belong to the distribution of species abundance of microbial communities. The major phyla (>0.1 %) of the anaerobes (e) immobilized on nano-composite. The size of the circle is proportional to the relative abundance of phyla in the fermentation medium. The color scale indicates the normalized relative abundances of phyla.

## 5. Conclusions

Hydrogen energy productivity from dark fermentation of delignified duckweed (DDW) is a big challenge due to its adversely impact on the environment. The anaerobes immobilized on nG/HAP successfully improved and promoted the hydrogen yield (HY). The HY was only 1.35 L/kgDW for dark fermentation of the native duckweed which was increased up to 21.05 L/kgDW for hydrogenation of delignified duckweed (DDW). The DDW was further provided a high HY with

supplementation of different doses of nG/HAP. The HY amounted to  $39.7 \pm 2.1$  and  $32.4 \pm 1.1$  L/kgDW for anaerobes supplemented with 80 and 120 mg/gVS of nG/HAP. These values were quite higher by values of 46 and 34 % as compared to batches supplemented with 10 and 30 mg/gVS of nG/HAP respectively. Data displayed that all samples were dominated by the phyla *Firmicutes* (27.55 %), *Proteobacteria* (34.53 %), *Actinobacteria* (9.44 %), *Bacteroidetes* (3.82 %), *Chloroflexi* (10.19 %) and *Planctomycetes* (6.64 %).

## CRediT authorship contribution statement

**Ahmed Tawfik:** Conceptualization, Writing – original draft, Formal analysis, Investigation, Methodology. **Xuefei Tan:** Project administration, Writing – review & editing, Funding acquisition. **Mohamed Elsa-madony:** Writing – review & editing. **Muhammad Abdul Qyyum:** Writing – review & editing. **Ahmed M. Azzam:** Writing – review & editing. **Muhammad Mubashir:** Writing – review & editing. **Hui Suan Ng:** Writing – review & editing. **Muhammad Saeed Akhtar:** Project administration, Resources, Writing – review & editing, Supervision. **Kuan Shiong Khoo:** Project administration, Supervision, Visualization, Writing – review & editing.

## Declaration of Competing Interest

The authors declare that they have no known competing financial interests or personal relationships that could have appeared to influence the work reported in this paper.

## Acknowledgements

The 1<sup>st</sup> author acknowledged the Science Technology Innovation Funding Agency (STIFA) – Egypt (Project ID: 41591) for fully financially supporting this research and bilateral research project between academy of Scientific Research and Technology (ASRT)-Egypt and National Natural Science Foundation of China. The 1<sup>st</sup> author is grateful to the National Research Centre-Egypt for partially supporting this research (Project ID: 12030202). This study was partially funded by University Nursing Program for Young Scholars with Creative Talents in Heilongjiang Province (No. UNPYSC-2020050), Heilongjiang Institute of Technology Doctoral Research Fund (2017BJ31), Provincial Leading Talent Echelon Cultivation Project of Heilongjiang Institute of Technology (No. 2020LJ03). Authors also acknowledged the Asia Pacific University of Technology & innovation, Malaysia for the support.

## References

- [1] Allam A, Tawfik A, Yoshimura C. Phytoremediation of Drainage Water Containing Mono Ethylene Glycol Using a Duckweed (*Lemna gibba*) Pond System. *J Environ Eng* 2016;142(5).
- [2] Tawfik A, Niaz H, Qadeer K, Qyyum MA, Liu JJ, Lee M. Valorization of algal cells for biomass and bioenergy production from wastewater: Sustainable strategies, challenges, and techno-economic limitations. *Renew Sustain Energy Rev* 2022;157: 112024. <https://doi.org/10.1016/j.rser.2021.112024>.
- [3] Osama R, Awad HM, Ibrahim MG, Tawfik A. Mechanistic and economic assessment of polyester wastewater treatment via baffled duckweed pond. *J Water Process Eng* 2020;35:101179.
- [4] Osama R, Ibrahim MG, Fujia M, Tawfik A. Potentials of duckweed (*Lemna gibba*) for treatment of 1,4-dioxane containing wastewater using duckweed multi-ponds system. *Energy Procedia* 2019;157:676–82.
- [5] Kreider AN, Fernandez Pulido CR, Bruns MA, Brennan RA. Duckweed as an Agricultural Amendment: Nitrogen Mineralization, Leaching, and Sorghum Uptake. *J Environ Qual* 2019;48:469–75. <https://doi.org/10.2134/jeq2018.05.0207>.
- [6] Bassuney D, Tawfik A. Baffled duckweed pond system for treatment of agricultural drainage water containing pharmaceuticals. *Int J Phytoremediation* 2017;19(8): 774–80.
- [7] Allam A, Tawfik A, El-Saadi A, Negm A. Potentials of using duckweed (*Lemna gibba*) for treatment of drainage water for reuse in irrigation purposes. *Desalin Water Treat* 2016;57. <https://doi.org/10.1080/19443994.2014.966760>.
- [8] Osama R, Awad HM, Zha S, Meng F, Tawfik A. Greenhouse gases emissions from duckweed pond system treating polyester resin wastewater containing 1,4-dioxane

- and heavy metals. *Ecotoxicol Environ Saf* 2021;207:111253. <https://doi.org/10.1016/j.ecoenv.2020.111253>.
- [9] Allam A, Tawfik A, Negm A, Yoshimura C, Fleifle A. Treatment of Drainage Water Containing Pharmaceuticals Using Duckweed (*Lemna gibba*). *Energy Procedia* 2015;74:973–80.
- [10] Verma R, Suthar S. Synchronized urban wastewater treatment and biomass production using duckweed *Lemna gibba* L. *Ecol Eng* 2014;64:337–43. <https://doi.org/10.1016/j.ecoleng.2013.12.055>.
- [11] Zheng Y, Zhao J, Xu F, Li Y. Pretreatment of lignocellulosic biomass for enhanced biogas production. *Prog Energy Combust Sci* 2014;42:35–53. <https://doi.org/10.1016/j.pecs.2014.01.001>.
- [12] Soltan M, Elsamadony M, Mostafa A, Awad H, Tawfik A. Nutrients balance for hydrogen potential upgrading from fruit and vegetable peels via fermentation process. *J Environ Manage* 2019;242:384–93. <https://doi.org/10.1016/j.jenvman.2019.04.066>.
- [13] Wazeri A, Elsamadony M, Tawfik A. Carbon emissions reduction by catalyzing H<sub>2</sub> gas harvested from water hyacinth fermentation process using metallic salts. *Energy Procedia* 2018;152:1254–9. <https://doi.org/10.1016/j.egypro.2018.09.178>.
- [14] Wazeri A, Elsamadony M, Le RS, Peu P, Tawfik A. Potentials of using mixed culture bacteria incorporated with sodium bicarbonate for hydrogen production from water hyacinth. *Bioresour Technol* 2018;263:365–74. <https://doi.org/10.1016/j.biotech.2018.05.021>.
- [15] Elsharkawy K, Gar Alalm M, Fujii M, Afify H, Tawfik A, Elsamadony M. Paperboard mill wastewater treatment via combined dark and LED-mediated fermentation in the absence of external chemical addition. *Bioresour Technol* 2020;295:122312. <https://doi.org/10.1016/j.biotech.2019.122312>.
- [16] Elsamadony M, Mostafa A, Fujii M, Tawfik A, Pant D. Advances towards understanding long chain fatty acids-induced inhibition and overcoming strategies for efficient anaerobic digestion process. *Water Res* 2021;190:116732.
- [17] Verma R, Suthar S. Utility of Duckweeds as Source of Biomass Energy: a Review. *Bioenergy Res* 2015;8:1589–97. <https://doi.org/10.1007/s12155-015-9639-5>.
- [18] Muradov N, Fidalgo B, Gujar AC, T-Raiissi A. Pyrolysis of fast-growing aquatic biomass – *Lemna minor* (duckweed). Characterization of pyrolysis products. *Bioresour Technol* 2010;101:8424–8. <https://doi.org/10.1016/j.biotech.2010.05.089>.
- [19] Gaur RZ, Khan AA, Suthar S. Effect of thermal pre-treatment on co-digestion of duckweed (*Lemna gibba*) and waste activated sludge on biogas production. *Chemosphere* 2017;174:754–63. <https://doi.org/10.1016/j.chemosphere.2017.01.133>.
- [20] Nasr M, Tawfik A, Awad HM, Galal A, El-Qelish M, Abdul Qyyum M, et al. Dual production of hydrogen and biochar from industrial effluent containing phenolic compounds. *Fuel* 2021;301:121087.
- [21] Tawfik A, Nasr M, Galal A, El-Qelish M, Yu Z, Hassan MA, et al. Fermentation-based nanoparticle systems for sustainable conversion of black-liquor into biogas. *J Clean Prod* 2021;309:127349.
- [22] Tawfik A, Elsamadony M. Development of Dry Anaerobic Technologies of Bio-waste and Unlock the Barriers for Valorization. In: Purohit HJ, Kalia VC, Vaidya AN, Khardenavis AA, editors. *Optim. Appl. Bioprocesses*. Singapore: Springer Singapore; 2017, pp. 267–82. [https://doi.org/10.1007/978-981-10-6863-8\\_13](https://doi.org/10.1007/978-981-10-6863-8_13).
- [23] Wang Y, Xi B, Li M, Jia X, Wang X, Xu P, et al. Hydrogen production performance from food waste using piggery anaerobic digested residues inoculum in long-term systems. *Int J Hydrogen Energy* 2020;45(58):33208–17.
- [24] Xu J, Deshusses MA. Fermentation of swine wastewater-derived duckweed for biogas production. *Int J Hydrogen Energy* 2015;40:7028–36. <https://doi.org/10.1016/j.ijhydene.2015.03.166>.
- [25] Tawfik A, Hassan GK, Awad H, Hassan M, Rojas P, Sanz JL, et al. Strengthen “the sustainable farm” concept via efficacious conversion of farm wastes into methane. *Bioresour Technol* 2021;341:125838.
- [26] Farghaly A, Elsamadony M, Ookawara S, Tawfik A. Bioethanol production from paperboard mill sludge using acid-catalyzed choline acetate ionic liquid pretreatment followed by fermentation process. *Energy Convers Manag* 2017;145:255–64. <https://doi.org/10.1016/j.enconman.2017.05.004>.
- [27] Elsharkawy K, Elsamadony M, Afify H. Comparative analysis of common full scale reactors for dry anaerobic digestion process. E3S Web Conf., vol. 83; 2019. p. 01011.
- [28] Elsamadony M. Enrich waste activated sludge digestibility via natural enzyme supplementation. E3S Web Conf., vol. 83; 2019. p. 01012.
- [29] Soltan M, Elsamadony M, Mostafa A, Awad H, Tawfik A. Harvesting zero waste from co-digested fruit and vegetable peels via integrated fermentation and pyrolysis processes. *Environ Sci Pollut Res* 2019;26(10):10429–38.
- [30] Tawfik A, El-Bery H, Elsamadony M, Kumari S, Bux F. Upgrading continuous H<sub>2</sub> gas recovery from rice straw hydrolysate via fermentation process amended with magnetite nanoparticles. *Int J Energy Res* 2019;43:3516–27. <https://doi.org/10.1002/er.4495>.
- [31] Mostafa A, Im S, Song Y-C, Park J-H, Kim S-H, Lim K-H, et al. Unravelling the enhancement of biogas production via adding magnetite nanoparticles and applying electrical energy input. *Int J Hydrogen Energy* 2021;1–9. <https://doi.org/10.1016/j.ijhydene.2021.08.117>.
- [32] Mostafa A, Kim M-G, Im S, Lee M-K, Kang S, Kim D-H. Series of combined pretreatment can affect the solubilization of waste-activated sludge. *Energies* 2020;13(16):4165.
- [33] Mostafa A, Im S, Song Y, Ahn Y, Kim D. Enhanced Anaerobic Digestion by Stimulating DIET Reaction. *Processes* 2020;8:424.
- [34] Mostafa A, Tolba A, Gar Alalm M, Fujii M, Afify H, Elsamadony M. Application of magnetic multi-wall carbon nanotube composite into fermentative treatment process of ultrasonicated waste activated sludge. *Bioresour Technol* 2020;306:123186.
- [35] Cheng J, Li H, Ding L, Zhou J, Song W, Li Y-Y, et al. Improving hydrogen and methane co-generation in cascading dark fermentation and anaerobic digestion: The effect of magnetite nanoparticles on microbial electron transfer and syntrophism. *Chem Eng J* 2020;397:125394.
- [36] Zhong D, Li J, Ma W, Xin H. Magnetite nanoparticles enhanced glucose anaerobic fermentation for bio-hydrogen production using an expanded granular sludge bed (EGSB) reactor. *Int J Hydrogen Energy* 2020;45:10664–72. <https://doi.org/10.1016/j.ijhydene.2020.01.095>.
- [37] Grosser A, Grobelak A, Rorat A, Courtois P, Vandenbulcke F, Lemière S, et al. Effects of silver nanoparticles on performance of anaerobic digestion of sewage sludge and associated microbial communities. *Renew Energy* 2021;171:1014–25.
- [38] Ajay CM, Mohan S, Dinesha P, Rosen MA. Review of impact of nanoparticle additives on anaerobic digestion and methane generation. *Fuel* 2020;277:118234. <https://doi.org/10.1016/j.fuel.2020.118234>.
- [39] Elreedy A, Ibrahim E, Hassan N, El-Dissouky A, Fujii M, Yoshimura C, et al. Nickel-graphene nanocomposite as a novel supplement for enhancement of biohydrogen production from industrial wastewater containing mono-ethylene glycol. *Energy Convers Manag* 2017;140:133–44.
- [40] Elreedy A, Fujii M, Koyama M, Nakasaki K, Tawfik A. Enhanced fermentative hydrogen production from industrial wastewater using mixed culture bacteria incorporated with iron, nickel, and zinc-based nanoparticles. *Water Res* 2019;151:349–61. <https://doi.org/10.1016/j.watres.2018.12.043>.
- [41] Salem AH, Mietzel T, Brunstermann R, Widmann R. Effect of cell immobilization, hematite nanoparticles and formation of hydrogen-producing granules on biohydrogen production from sucrose wastewater. *Int J Hydrogen Energy* 2017;42:25225–33. <https://doi.org/10.1016/j.ijhydene.2017.08.060>.
- [42] Mostafa A, El-Dissouky A, Fawzy A, Farghaly A, Peu P, Dabert P, et al. Magnetite/graphene oxide nano-composite for enhancement of hydrogen production from gelatinaceous wastewater. *Bioresour Technol* 2016;216:520–8.
- [43] Tawfik A, Hasanen K, Abdulla M, Badr OA, Awad HM, Elsamadony M, et al. Graphene enhanced detoxification of wastewater rich 4-nitrophenol in multistage anaerobic reactor followed by baffled high-rate algal pond. *J Hazard Mater* 2022;424:127395.
- [44] Kaur M, Sahoo PC, Kumar M, Sachdeva S, Puri SK. Effect of metal nanoparticles on microbial community shift and syntrophic metabolism during anaerobic digestion of Azolla microphylla. *J Environ Chem Eng* 2021;9(5):105841.
- [45] Hassan MA, Mohammad AM, Salaheldin TA, El-Anadolli BE. A promising hydroxyapatite/graphene hybrid nanocomposite for methylene blue dye's removal in wastewater treatment. *Int J Electrochem Sci* 2018;13:8222–40. <https://doi.org/10.20964/2018.08.77>.
- [46] Kahrizi P, Mohseni-Shahri FS, Moeinpour F. Adsorptive removal of cadmium from aqueous solutions using NiFe204/hydroxyapatite/graphene quantum dots as a novel nano-adsorbent. *J Nanostruct Chem* 2018;8:441–52. <https://doi.org/10.1007/s40097-018-0284-3>.
- [47] Turon P, del Valle L, Alemán C, Puiggall J. Biodegradable and biocompatible systems based on hydroxyapatite nanoparticles. *Appl Sci* 2017;7(1):60.
- [48] Wen T, Wu X, Liu M, Xing Z, Wang X, Xu AW. Efficient capture of strontium from aqueous solutions using graphene oxide-hydroxyapatite nanocomposites. *Dalt Trans* 2014;43:7464–72. <https://doi.org/10.1039/c3dt53591f>.
- [49] Bharath G, Ponpandian N. Hydroxyapatite nanoparticles on dendritic α-Fe2O3 hierarchical architectures for a heterogeneous photocatalyst and adsorption of Pb (II) ions from industrial wastewater. *RSC Adv* 2015;5:84685–93. <https://doi.org/10.1039/c5ra15703j>.
- [50] Safatian F, Doago Z, Torabbeigi M, Rahmani Shams H, Ahadi N. Lead ion removal from water by hydroxyapatite nanostructures synthesized from egg shells with microwave irradiation. *Appl Water Sci* 2019;9:1–6. <https://doi.org/10.1007/s13201-019-0979-8>.
- [51] Pu Y, Tang J, Wang XC, Hu Y, Huang J, Zeng Y, et al. Hydrogen production from acidogenic food waste fermentation using untreated inoculum: Effect of substrate concentrations. *Int J Hydrogen Energy* 2019;44(50):27272–84.
- [52] Hendi AA, Yakuphanoglu F. Dielectric and ferroelectric properties of the graphene doped hydroxyapatite ceramics. *J Mol Struct* 2020;1207:127734. <https://doi.org/10.1016/j.molstruc.2020.127734>.
- [53] Mishra P, Ameen F, Zaid RM, Singh L, Wahid ZA, Islam MA, et al. Relative effectiveness of substrate-inoculum ratio and initial pH on hydrogen production from palm oil mill effluent: Kinetics and statistical optimization. *J Clean Prod* 2019;228:276–83.
- [54] Mazareli RCDS, Villa Montoya AC, Delforno TP, Centurion VB, de Oliveira VM, Silva EL, et al. Enzymatic routes to hydrogen and organic acids production from banana waste fermentation by autochthonous bacteria: Optimization of pH and temperature. *Int J Hydrogen Energy* 2021;46(12):8454–68.
- [55] Mu D, Liu H, Lin W, Shukla P, Luo J. Simultaneous biohydrogen production from dark fermentation of duckweed and waste utilization for microalgal lipid production. *Bioresour Technol* 2020;302:122879. <https://doi.org/10.1016/j.biotech.2020.122879>.
- [56] Van Soest PJ, Wine RH. Determination of Lignin and Cellulose in Acid-Detergent Fiber with Permanganate. *J AOAC Int* 1968;51:780–5. <https://doi.org/10.1093/jaoac/51.4.780>.
- [57] APHA. Standard Methods for the Examination of Water and Wastewater. 25th Ed Washington, DC Am Public Heal Assoc Water Work Assoc Water Environ Fed; 2005.
- [58] Miller GL. Use of Dinitrosalicylic Acid Reagent for Determination of Reducing Sugar. *Anal Chem* 1959;31:426–8. <https://doi.org/10.1021/ac60147a030>.

- [59] Velioglu YS, Mazza G, Gao L, Oomah BD. Antioxidant Activity and Total Phenolics in Selected Fruits, Vegetables, and Grain Products. *J Agric Food Chem* 1998;46: 4113–7. <https://doi.org/10.1021/jf9801973>.
- [60] DuBois M, Gilles KA, Hamilton JK, Rebers PA, Smith F. Colorimetric method for determination of sugars and related substances. *Anal Chem* 1956;28(3):350–6.
- [61] Lee D, Li Y, Oh Y, Kim M, Noike T. Effect of iron concentration on continuous H<sub>2</sub> production using membrane bioreactor. *Int J Hydrogen Energy* 2009;34:1244–52. <https://doi.org/10.1016/j.ijhydene.2008.11.093>.
- [62] Emami Bistgani Z, Siadat SA, Bakhshandeh A, Ghasemi Pirbalouti A, Hashemi M. Interactive effects of drought stress and chitosan application on physiological characteristics and essential oil yield of Thymus daenensis Celak. *Crop J* 2017;5: 407–15. <https://doi.org/10.1016/j.cj.2017.04.003>.
- [63] Delbès C, Moletta R, Godon JJ. Bacterial and archaeal 16S rDNA and 16S rRNA dynamics during an acetate crisis in an anaerobic digester ecosystem. *FEMS Microbiol Ecol* 2001;35:19–26. [https://doi.org/10.1016/S0168-6496\(00\)00107-0](https://doi.org/10.1016/S0168-6496(00)00107-0).
- [64] Poirier S, Desmond-Le Quéméner E, Madigou C, Bouchez T, Chapleur O. Anaerobic digestion of biowaste under extreme ammonia concentration: Identification of key microbial phylotypes. *Bioresour Technol* 2016;207:92–101. <https://doi.org/10.1016/j.biortech.2016.01.124>.
- [65] Wu H, Irizarry RA, Bravo HC. Intensity normalization improves color calling in SOLiD sequencing. *Nat Methods* 2010;7:336–7. <https://doi.org/10.1038/nmeth.0510-336>.
- [66] Edgar RC. UPARSE: Highly accurate OTU sequences from microbial amplicon reads. *Nat Methods* 2013;10:996–8. <https://doi.org/10.1038/nmeth.2604>.
- [67] Schloss PD, Westcott SL, Ryabin T, Hall JR, Hartmann M, Hollister EB, et al. Introducing mothur: Open-source, platform-independent, community-supported software for describing and comparing microbial communities. *Appl Environ Microbiol* 2009;75(23):7537–41.
- [68] Edgar RC. Search and clustering orders of magnitude faster than BLAST. *Bioinformatics* 2010;26:2460–1. <https://doi.org/10.1093/bioinformatics/btq461>.
- [69] Oksanen J, Blanchet F, Kindt R, Legendre P, O'hara R, Simpson G, et al. vegan: Community Ecology Package. R package version 1.17-12. R Foundation for Statistical Computing, Vienna, Austria 2011.
- [70] Wang Q, Garrity GM, Tiedje JM, Cole JR. Naïve Bayesian classifier for rapid assignment of rRNA sequences into the new bacterial taxonomy. *Appl Environ Microbiol* 2007;73:5261–7. <https://doi.org/10.1128/AEM.00062-07>.
- [71] Li Z, Cai W, Liu J, Zhou M, Cheng L, Yu H, et al. One-pot exfoliation and synthesis of hydroxypapatite-functionalized graphene as multifunctional nanomaterials based on electrochemical approach. *Compos Part A Appl Sci Manuf* 2021;149:106583.
- [72] Fang F, Huo S, Shen H, Ran S, Wang H, Song P, et al. A bio-based ionic complex with different oxidation states of phosphorus for reducing flammability and smoke release of epoxy resins. *Compos Commun* 2020;17:104–8.
- [73] Sawatdeenarunat C, Surendra KC, Takara D, Oechsner H, Khanal SK. Anaerobic digestion of lignocellulosic biomass: Challenges and opportunities. *Bioresour Technol* 2015;178:178–86.
- [74] Chang FY, Lin CY. Calcium effect on fermentative hydrogen production in an anaerobic up-flow sludge blanket system. *Water Sci Technol* 2006;54:105–12. <https://doi.org/10.2166/wst.2006.867>.
- [75] Kosaric N, Blaszczyk R, Orphan L. Factors influencing formation and maintenance of granules in anaerobic sludge blanket reactors (UASBR). *Water Sci Technol* 1990; 22:275–82. <https://doi.org/10.2166/wst.1990.0092>.
- [76] Nasr M, Tawfik A, Ookawara S, Suzuki M, Kumari S, Bux F. Continuous biohydrogen production from starch wastewater via sequential dark-photo fermentation with emphasize on maghemite nanoparticles. *J Ind Eng Chem* 2015; 21:500–6.
- [77] Zhao W, Zhao J, Chen G, Feng R, Yang J, Zhao Y, et al. Anaerobic biohydrogen production by the mixed culture with mesoporous Fe3O4 nanoparticles activation. *Adv Mater Res* 2011;306–307:1528–31. <https://doi.org/10.4028/www.scientific.net/AMR.306-307.1528>.
- [78] Malik SN, Pugalenthhi V, Vaidya AN, Ghosh PC, Mudliar SN. Kinetics of nano-catalysed dark fermentative hydrogen production from distillery wastewater. *Energy Proc* 2014;54:417–30. <https://doi.org/10.1016/j.egypro.2014.07.284>.
- [79] Han H, Cui M, Wei L, Yang H, Shen J. Enhancement effect of hematite nanoparticles on fermentative hydrogen production. *Bioresour Technol* 2011;102: 7903–9. <https://doi.org/10.1016/j.biortech.2011.05.089>.
- [80] Yuan Z, Yang H, Zhi X, Shen J. Increased performance of continuous stirred tank reactor with calcium supplementation. *Int J Hydrogen Energy* 2010;35:2622–6. <https://doi.org/10.1016/j.ijhydene.2009.04.018>.
- [81] Gadhe A, Sonawane SS, Varma MN. Enhancement effect of hematite and nickel nanoparticles on biohydrogen production from dairy wastewater. *Int J Hydrogen Energy* 2015;40:4502–11. <https://doi.org/10.1016/j.ijhydene.2015.02.046>.
- [82] Gadhe A, Sonawane SS, Varma MN. Influence of nickel and hematite nanoparticle powder on the production of biohydrogen from complex distillery wastewater in batch fermentation. *Int J Hydrogen Energy* 2015;40:10734–43. <https://doi.org/10.1016/j.ijhydene.2015.05.198>.
- [83] Mshandete A, Björnsson L, Kivaisi AK, Rubindamayugi ST, Mattiasson B. Enhancement of anaerobic batch digestion of sisal pulp waste by mesophilic aerobic pre-treatment. *Water Res* 2005;39:1569–75. <https://doi.org/10.1016/j.watres.2004.11.037>.
- [84] Parawira W. Enzyme research and applications in biotechnological intensification of biogas production. *Crit Rev Biotechnol* 2012;32:172–86. <https://doi.org/10.3109/07388551.2011.595384>.
- [85] Morgan JW, Evison LM, Forster CF. Changes to the microbial ecology in anaerobic digesters treating ice cream wastewater during start-up. *Water Res* 1991;25: 639–53. [https://doi.org/10.1016/0043-1354\(91\)90039-S](https://doi.org/10.1016/0043-1354(91)90039-S).
- [86] Bagi Z, Ács N, Bálint B, Horváth L, Dobó K, Perei KR, et al. Biotechnological intensification of biogas production. *Appl Microbiol Biotechnol* 2007;76(2): 473–82.
- [87] Feng Y, Zhang Y, Quan X, Chen S. Enhanced anaerobic digestion of waste activated sludge digestion by the addition of zero valent iron. *Water Res* 2014;52:242–50. <https://doi.org/10.1016/j.watres.2013.10.072>.
- [88] Roman HJ, Burgess JE, Pletschke BI. Enzyme treatment to decrease solids and improve digestion of primary sewage sludge. *African J Biotechnol* 2006;5:963–7. <https://doi.org/10.5897/AJB06.154>.
- [89] Luo K, Yang Qi, Li X-M, Yang G-J, Liu Y, Wang D-b, et al. Hydrolysis kinetics in anaerobic digestion of waste activated sludge enhanced by α-amylase. *Biochem Eng J* 2012;62:17–21.
- [90] Zeng Z, Li Y, Yang R, Liu C, Hu X, Luo S, et al. The relationship between reducing sugars and phenolic retention of brown rice after enzymatic extrusion. *J Cereal Sci* 2017;74:244–9.
- [91] Hernandez JE, Edyvean RGJ. Inhibition of biogas production and biodegradability by substituted phenolic compounds in anaerobic sludge. *J Hazard Mater* 2008;160: 20–8. <https://doi.org/10.1016/j.jhazmat.2008.02.075>.
- [92] Yuan Z, Yang H, Zhi X, Shen J. Enhancement effect of l-cysteine on dark fermentative hydrogen production. *Int J Hydrogen Energy* 2008;33:6535–40. <https://doi.org/10.1016/j.ijhydene.2008.07.065>.
- [93] Tawfik A, Hassan GK, Awad H, Hassan M, Rojas P, Sanz JL, et al. Strengthen “the sustainable farm” concept via efficacious conversion of farm wastes into methane. *Bioresour Technol* 2021;341:125838.
- [94] Poirier S, Bize A, Bureau C, Bouchez T, Chapleur O. Community shifts within anaerobic digestion microbiota facing phenol inhibition: Towards early warning microbial indicators? *Water Res* 2016;100:296–305. <https://doi.org/10.1016/j.watres.2016.05.041>.
- [95] Awasthi A, Singh M, Soni SK, Singh R, Kalra A. Biodiversity acts as insurance of productivity of bacterial communities under abiotic perturbations. *ISME J* 2014;8: 2445–52. <https://doi.org/10.1038/ismej.2014.91>.
- [96] Ventura M, Canchaya C, Tauch A, Chandra G, Fitzgerald GF, Chater KF, et al. Genomics of Actinobacteria : Tracing the Evolutionary History of an Ancient Phylum. *Microbiol Mol Biol Rev* 2007;71:495–548. <https://doi.org/10.1128/mmbr.00005-07>.